

A measurement of electroweak effects in the reaction $e^+e^- \rightarrow \tau^+\tau^-$ at 35.0 and 42.4 GeV

TASSO Collaboration

W. Braunschweig, R. Gerhards, F.J. Kirschfink¹,
H.-U. Martyn
I. Physikalisches Institut der RWTH Aachen, D-5100 Aachen,
Federal Republic of Germany^a

H.M. Fischer, H. Hartmann, J. Hartmann,
E. Hilger, A. Jocksch, R. Wedemeyer
Physikalisches Institut der Universität Bonn, D-5300 Bonn,
Federal Republic of Germany^a

B. Foster, A.J. Martin
H.H. Wills Physics Laboratory, University of Bristol,
Bristol BS8 1TL, UK^b

E. Bernardi, J. Chwastowski², K. Gather,
K. Genser³, H. Kowalski, B. Löhr, D. Lüke,
D. Notz, J.M. Pawlak³, K.-U. Pösnecker, E. Ros,
R. Walczak³, G. Wolf
Deutsches Elektronen-Synchrotron, DESY, D-2000 Hamburg,
Federal Republic of Germany

H. Kolanoski
Institut für Physik, Universität Dortmund, D-4600 Dortmund,
Federal Republic of Germany

J. Krüger, E. Lohrmann, G. Poelz, W. Zeuner⁴
II. Institut für Experimentalphysik der Universität Hamburg,
D-2000 Hamburg, Federal Republic of Germany^a

J. Hassard, J. Shulman, D. Su⁵, I.R. Tomalin
Department of Physics, Imperial College, London SW7 2AZ,
UK^b

F. Barreiro, A. Leites, J. del Peso, M. Traseira
Universidad Autonoma de Madrid, Madrid, Spain^c

C. Balkwill, M.G. Bowler, P.N. Burrows⁶,
R.J. Cashmore, G.P. Heath, P.N. Ratoff,
I.M. Silvester, M.E. Veitch
Department of Nuclear Physics, Oxford University,
Oxford OX1 3RH, UK^b

J.C. Hart, D.H. Saxon
Rutherford Appleton Laboratory, Chilton, Didcot,
Oxon OX11 0QX, UK^b

S. Brandt, M. Holder
Fachbereich Physik der Universität-Gesamthochschule Siegen,
D-5900 Siegen, Federal Republic of Germany^a

Y. Eisenberg, U. Karshon, G. Mikenberg,
A. Montag, D. Revel, E. Ronat, A.N. Wainer,
G. Yekutieli
Weizmann Institute, Rehovot 76100, Israel^d

D. Muller, S. Ritz, M. Takashima, Sau Lan Wu,
G. Zoernig
Department of Physics, University of Wisconsin,
Madison, WI 53706, USA^e

Received 23 March 1989

¹ Now at Lufthansa, Hamburg, FRG

² Now at Inst. of Nuclear Physics, Cracow, Poland

³ Now at Warsaw University, Poland

⁴ Now at CERN, Geneva, Switzerland

⁵ Now at Rutherford Appleton Laboratory, Chilton, UK

⁶ Now at MIT, Cambridge, USA

^a Supported by the Bundesministerium für Forschung und Technologie

^b Supported by the UK Science and Engineering Research Council

^c Supported by CAICYT

^d Supported by the Minerva Gesellschaft für Forschung mbH

^e Supported by the US Dept. of Energy, contract DE-AC02-76ER00881 and by the US National Science Foundation Grant no. INT-8313994 for travel

Abstract. We report on total cross section and forward backward charge asymmetry measurements of the reaction $e^+e^- \rightarrow \tau^+\tau^-$ at centre of mass energies of 35.0 GeV and 42.4 GeV using the TASSO detector. Including previous data an analysis in terms of electroweak parameters of the standard model is presented, and lower limits on mass scale parameters of residual contact interactions are given. A combined analysis of electroweak couplings using all our results on leptonic reactions $e^+e^- \rightarrow l^+l^-$ has been performed.

1 Introduction

In this paper we present a study of the production characteristics of the reaction $e^+e^- \rightarrow \tau^+\tau^-$ using the TASSO detector at the PETRA storage ring. The data were collected during an energy scan between 38.3 and 46.8 GeV centre of mass energy at an average energy of $\sqrt{\langle s \rangle} = 42.4$ GeV with a total integrated luminosity of $\int \mathcal{L} dt = 44.0 \text{ pb}^{-1}$ and at a fixed energy of $\sqrt{s} = 35.0$ GeV with an integrated luminosity of $\int \mathcal{L} dt = 108.6 \text{ pb}^{-1}$. This is a continuation of our previous analysis of τ pair production [1] at similar and lower energies.

The reaction $e^+e^- \rightarrow \tau^+\tau^-$ provides a clean test of the electroweak sector of the standard model [2]. The interference of the photon and the Z^0 pole leads at PETRA energies to a substantial forward backward asymmetry in the differential cross section of the τ pairs. The effect of Z^0 exchange on the total cross section is, however, still small (less than $\sim 1\%$) and the total cross section measurement therefore provides a test of QED. The electroweak parameters determined in tau pair production are compared to those derived from the light leptons, muons and electrons, and used to perform a combined analysis.

2 Event selection

The TASSO detector has been described in detail elsewhere [3, 4] and here we simply note that the information used in the trigger and event selection was taken from the inner tracking chambers (a vertex detector, a proportional chamber and a drift chamber) and the surrounding time of flight scintillator counters. The analysis methods closely follow our previous publication [1]; more details can be found in [5, 6].

Events were selected in which one τ decayed into one charged track (+unobserved neutrals) and the other τ into three charged tracks (+unobserved neutrals), the 1–3 τ pair topology; no particle identification was attempted. This distinctive topology is characteristic for about a quarter of all τ pair decays, but allows one to prepare a very clean event sample.

Candidate events were required to have four well reconstructed tracks originating from a common event vertex (a cylinder of 2 cm radius and 20 cm length around the nominal interaction point), contained within the detector (polar angle $|\cos \theta| \leq 0.82$) and having a total charge of zero. The angle between any two tracks of the three particles forming a jet of one τ decay was required to be less than 30° (25° for $\sqrt{s} > 38$ GeV) and the angle between the lone track

and any other track to be greater than 100° . These cuts effectively removed hadronic events. Two photon events $e^+e^- \rightarrow e^+e^-\tau^+\tau^-$ were removed by a cut on the scalar momentum sum in the event ($\sum |\mathbf{p}_i| > 0.4 p_{\text{beam}}$, where p_{beam} is the beam momentum).

A serious background comes from Bhabha scattering events with a radiated photon converted into an e^+e^- pair in the beam pipe or tracking chambers material, thus faking a 3-prong τ decay. The production cross section is very large and strongly peaked in the forward direction. To reduce this background acollinearity cuts (the angle between the momentum of the lone track and the momentum vector of the 3 tracks had to be less than 179°) and momentum cuts (the momentum of the lone track had to be $p_{\text{lone}} < 0.97 p_{\text{beam}}$, and the momentum of each track of the 3 particle system $p_{i,\text{jet}} < 0.90 p_{\text{beam}}$) were applied. Furthermore photon conversions were searched for. If two oppositely charged tracks in a jet had a common intersection point close to the beam pipe or inside the tracking chambers and their invariant mass, assuming electron masses for both tracks, was less than 150 MeV the event was rejected.

The polar angle of a τ pair event was defined as $\cos \bar{\theta} = \mathbf{e}^+ \cdot (\boldsymbol{\tau}^+ - \boldsymbol{\tau}^-) / |\mathbf{e}^+| |\boldsymbol{\tau}^+ - \boldsymbol{\tau}^-|$, where \mathbf{e}^+ is the positron momentum and $\boldsymbol{\tau}^+$ and $\boldsymbol{\tau}^-$ are the momenta of the lone track or the 3 particle jet. Only events with $|\cos \bar{\theta}| < 0.80$ were retained.

The final data samples contain 476 events at $\sqrt{s} = 35.0$ GeV and 117 events at $\sqrt{\langle s \rangle} = 42.4$ GeV.

3 Measurement of efficiencies

The events were required to set the coplanar trigger [3, 4], which was formed by at least two charged track candidates having an acoplanarity angle measured in the plane perpendicular to the beam direction of less than 27° for most of the 35 GeV data and some of the high energy data and less than 13° for the rest of the data (the cut was varied in order to reduce the number of triggers due to noise). A track candidate at the trigger level was formed by requiring connected information from the hits in the inner tracking chambers associated with a corresponding hit in one of the 48 time of flight counters.

The probability that a particle forms a track candidate in the tracking chambers was measured using Bhabha scattering events which were triggered and selected using shower counter information only. The time of flight counter efficiency was measured using hadronic data [6, 7]. To allow for the acollinearity between tracks from different τ decays, Monte Carlo $e^+e^- \rightarrow \tau^+\tau^-$ events were generated and the trigger logic was simulated.

The efficiencies varied throughout the data taking period, but the overall trigger efficiency for 1–3 τ pair events satisfying the selection criteria was typically $\sim 90\%$, and, most important, did not show any significant polar angle dependence.

The selection efficiency for $e^+e^- \rightarrow \tau^+\tau^-$ events was determined using Monte Carlo techniques. Tau pair events were generated and passed through a detector simulation, and the same reconstruction programs and cuts were applied as to the data. The overall selection efficiency was found to be typically $\sim 8\%$, including branching fractions, geometrical acceptance and efficiencies. The polar angle dependence of the selection efficiency was found to be constant except for small geometrical acceptance corrections beyond $|\cos \bar{\theta}| > 0.70$.

4 Backgrounds

The background in the τ pair data from hadronic and two photon events was estimated using Monte Carlo techniques. The contamination from hadronic events is calculated to be $(3.0 \pm 1.1)\%$ at 35.0 GeV and $(1.5 \pm 1.1)\%$ at 42.4 GeV. The two photon background from $e^+e^- \rightarrow e^+e^- + \text{hadrons}$ was found to be negligible at both energies, and from $e^+e^- \rightarrow e^+e^-\tau^+\tau^-$ was found to be $(1.7 \pm 0.2)\%$ at 35.0 GeV and $(2.0 \pm 0.3)\%$ at 42.4 GeV.

The background from Bhabha scattering events was estimated by several methods. First, Monte Carlo Bhabha event simulation suggested that the background was low, $(0.4 \pm 0.3)\%$. Secondly, events were searched for in the τ pair data sets in which the lone track as well as one of the jet tracks were identified as electrons in the calorimeters. One event was found which was also consistent with a genuine τ pair decay, where a photon overlaps with a charged track in the jet. Taking the limited acceptance and particle identification into account we expect a Bhabha background of $(0.4 \pm 0.4)\%$, consistent with the above Monte Carlo method.

The estimated background has been subtracted from the data for the total cross section determination and taken into account with its proper angular distribution in the asymmetry measurements.

5 Radiative corrections

The selection criteria described in Sect. 2 include radiative events of the type $e^+e^- \rightarrow \tau^+\tau^-\gamma$. In order to compare the measured cross sections and asymmetries with lowest order predictions and results from other experiments, radiative corrections have to be

applied to the data. The radiative correction function depends on the experimental cuts and has been determined by Monte Carlo simulation using a μ pair event generator [8] modified to produce τ pairs. All purely electromagnetic contributions up to order α^3 were included, known as ‘reduced QED’ radiative corrections [9]. Order α^3 weak corrections to both photon and Z^0 exchange diagrams were not included, as at the energies investigated their small contributions almost exactly cancel out order α^3 electromagnetic corrections to Z^0 exchange diagrams, which were also omitted [9]. Radiative processes modify the observed asymmetry by about $+1\%$. Due to the many unobserved particles (neutrinos and photons) the exact phase space of the accepted τ pairs is not well defined. This leads to a systematic uncertainty in the asymmetry measurement of $\pm 0.5\%$. All data presented include ‘reduced QED’ radiative corrections.

6 Systematic errors

The combined systematic error on the total cross section was $\pm 6.6\%$ at 35.0 GeV and $\pm 7.8\%$ at 42.4 GeV. The major contributions were from the uncertainties on the luminosity ($\sim 3\text{--}4\%$), the efficiencies ($\sim 4\text{--}5\%$), the background subtraction ($\sim 1\%$), and the branching ratios ($\sim 5\%$). The τ branching ratios were taken from [10] with all hadronic one prong decays scaled up, so that the sum of exclusive one prong branching fractions was equal to the measured inclusive one prong branching fraction. Other sources of systematic error, such as the uncertainty in the detector simulation, and the effect of varying the cuts within reasonable ranges were found to give much smaller contributions.

The systematic error from most of these sources does not affect the asymmetry. However there is a larger contribution from the uncertainty in the Bhabha background ($\Delta A = \pm 0.8\%$), and a smaller contribution from the uncertainty in the radiative corrections ($\Delta A = \pm 0.5\%$). The absolute systematic error on the forward backward asymmetry has been estimated to be ($\Delta A = \pm 1.0\%$). This estimate is consistent with a fit to the differential cross section without the highest $\cos \bar{\theta} > 0.6$ bin, where most of the Bhabha background is expected.

7 Results

The data were analysed in terms of electroweak parameters of the standard model [2]. In the standard model the lowest order differential cross section for

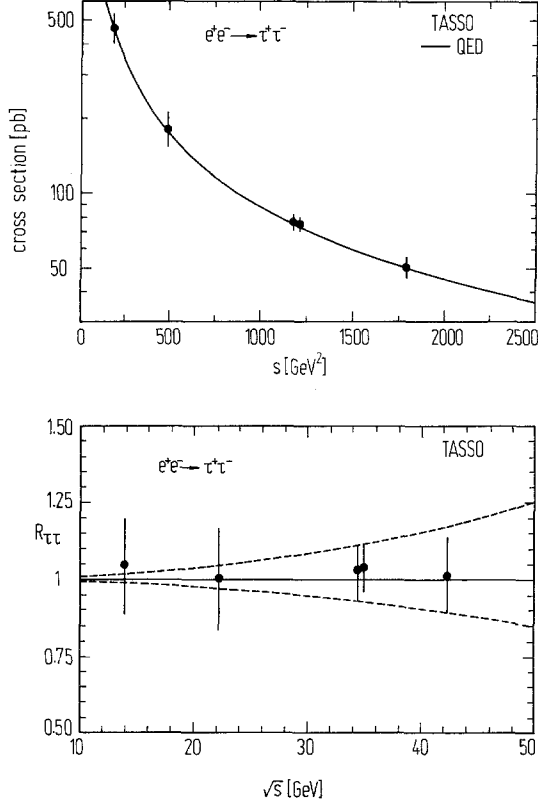


Fig. 1. **a** The total cross section for the reaction $e^+e^- \rightarrow \tau^+\tau^-$ as a function of s . The curve shows the QED prediction. **b** $R_{\tau\tau}$ as a function of \sqrt{s} . The curves show the expected deviations from QED for cut-off parameters $A_1^{\text{QED}} = 184$ GeV and $A_2^{\text{QED}} = 221$ GeV. The data points include statistical and systematic errors

$e^+e^- \rightarrow \tau^+\tau^-$ is given by

$$\frac{d\sigma}{d\Omega} = \frac{\alpha^2}{4s} (C_1(1 + \cos^2\theta) + C_2 \cos\theta), \quad (1)$$

where

$$C_1 = 1 + 2g_V^e g_V^\tau \text{Re}(\chi) + (g_V^{e2} + g_A^{e2})(g_V^{\tau2} + g_A^{\tau2})|\chi|^2 \quad (2)$$

and

$$C_2 = 4g_A^e g_A^\tau \text{Re}(\chi) + 8g_V^e g_V^\tau g_A^e g_A^\tau |\chi|^2. \quad (3)$$

$g_V^e, g_V^\tau, g_A^e, g_A^\tau$ are the vector and axial vector couplings of the electron and tau. In the standard model $g_A^e = g_A^\tau = -1/2$ and $g_V^e = g_V^\tau = -1/2 + 2 \sin^2 \theta_w$.

The function χ is given by the neutral current coupling, i.e. the weak mixing angle $\sin^2 \theta_w$, and the Z^0 propagator and has been parametrised as follows [11]:

$$\chi = \frac{1}{4 \sin^2 \theta_w \cos^2 \theta_w} \frac{s}{s - M_Z^2 + i M_Z \Gamma_Z}. \quad (4)$$

In this scheme the ‘reduced QED’ corrected data can be directly compared to the lowest order Born term calculations.

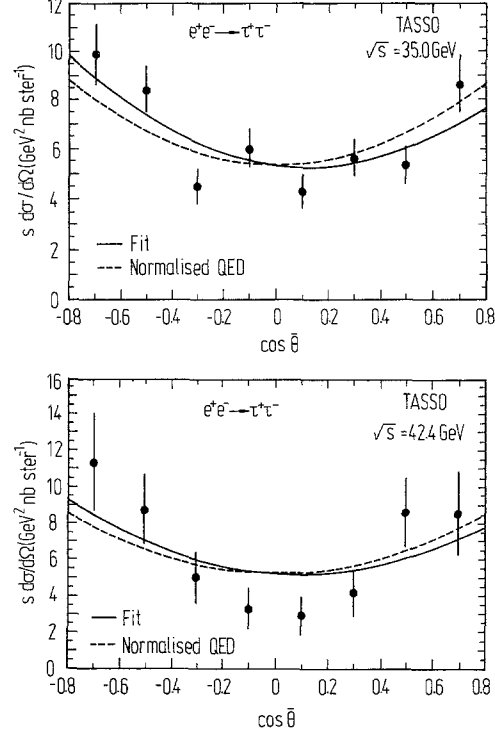


Fig. 2a, b. The differential cross section $s \frac{d\sigma}{d\Omega}$ for the reaction $e^+e^- \rightarrow \tau^+\tau^-$ at energies of **a** $\sqrt{s} = 35.0$ GeV and **b** $\sqrt{\langle s \rangle} = 42.4$ GeV. ‘Reduced QED’ corrections have been applied. The solid line shows the result of a fit to the standard model, the dashed line is the prediction of QED normalised to the observed total cross section. Statistical errors only are shown

The vector couplings are essentially determined by the total cross section, whereas the axial vector couplings are related to the forward backward charge asymmetry

$$A_{\tau\tau} = \frac{3C_2}{8C_1} \simeq \frac{3}{2} g_A^e g_A^\tau \text{Re}(\chi). \quad (5)$$

For numerical calculations we use $M_Z = (91.9 \pm 1.8)$ GeV [12], $\Gamma_Z = 2.8$ GeV and $\sin^2 \theta_w = 0.226 \pm 0.007$ [13]. This value of $\sin^2 \theta_w$ is in agreement with a more recent analysis of [14] using all neutrino nucleon deep inelastic scattering data.

The results on the total cross section at $\sqrt{s} = 35.0$ GeV and $\sqrt{\langle s \rangle} = 42.4$ GeV are shown in Fig. 1 and listed in Table 1 together with earlier TASSO data [1] (not included in the present data samples). We define $R_{\tau\tau} = \sigma_{\tau\tau} / \sigma^0$, where $\sigma_{\tau\tau}$ is the measured τ pair cross section with ‘reduced QED’ radiative corrections applied and σ^0 is the lowest order QED prediction. Our measurements are well described by QED. Even at the highest PETRA energy the predicted deviation of $R_{\tau\tau}$ from unity due to Z^0 exchange

Table 1. Data samples and results of total cross section and asymmetry measurements of the reaction $e^+e^- \rightarrow \tau^+\tau^-$. When two errors are given, the first is statistical and the second systematic, when only one error is given it is the sum of both added in quadrature. A_{GSW} is the standard model lowest order prediction with typical errors of $\pm 0.45\%$ at 35 GeV and $\pm 0.75\%$ at 42.4 GeV mostly due to the Z mass uncertainty

$\sqrt{\langle s \rangle}$ [GeV]	$\int \mathcal{L} dt$ [pb $^{-1}$]	$N_{\tau\tau}$	$\sigma_{\tau\tau}$ [pb]	$R_{\tau\tau}$	$A_{\tau\tau}$ [%]	A_{GSW} [%]
13.9	1.8	63	470 ± 60 -49	1.05 ± 0.14 -0.11	—	—
22.3	3.2	46	176 ± 26 -20	1.01 ± 0.15 -0.11	—	—
34.5	69.4	608	75 ± 4 -8	1.03 ± 0.05 -0.11	-4.9 ± 5.3 -1.2	-8.7
35.0	108.6	476	$73.4 \pm 3.5 \pm 4.8$	$1.036 \pm 0.050 \pm 0.068$	$-9.2 \pm 5.2 \pm 1.0$	-8.9
42.4	44.0	117	$48.8 \pm 4.7 \pm 3.8$	$1.011 \pm 0.097 \pm 0.079$	$-6.6 \pm 9.5 \pm 1.0$	-14.2

is only about 1%, well below the accuracy of the data.

The differential cross sections at $\sqrt{s}=35.0$ GeV and $\sqrt{\langle s \rangle}=42.4$ GeV are shown in Fig. 2 and listed in Table 2 (for convenience the old data at $\sqrt{\langle s \rangle}=34.5$ GeV are given as well). From a maximum like-

Table 2. The differential cross sections, $s \frac{d\sigma}{d\Omega}$, for the reaction $e^+e^- \rightarrow \tau^+\tau^-$ at centre of mass energies of 34.5, 35.0 and 42.4 GeV. ‘Reduced QED’ radiative corrections have been applied to the data. Statistical errors only are given; for systematic errors see text

$\cos \bar{\theta}$	$\sqrt{\langle s \rangle}=34.5$ GeV $s \frac{d\sigma}{d\Omega}$ [GeV 2 nb]	$\sqrt{s}=35.0$ GeV $s \frac{d\sigma}{d\Omega}$ [GeV 2 nb]	$\sqrt{\langle s \rangle}=42.4$ GeV $s \frac{d\sigma}{d\Omega}$ [GeV 2 nb]
-0.8-0.6	7.35 ± 1.13	9.90 ± 1.30	11.4 ± 2.7
-0.6-0.4	5.36 ± 0.79	8.46 ± 0.97	8.8 ± 2.0
-0.4-0.2	7.24 ± 0.79	4.53 ± 0.70	5.0 ± 1.4
-0.2-0.0	5.17 ± 0.64	6.04 ± 0.79	3.3 ± 1.2
0.0-0.2	5.85 ± 0.68	4.33 ± 0.67	2.9 ± 1.1
0.2-0.4	4.91 ± 0.64	5.69 ± 0.78	4.2 ± 1.3
0.4-0.6	5.48 ± 0.83	5.40 ± 0.78	8.7 ± 1.9
0.6-0.8	8.59 ± 1.28	8.76 ± 1.22	8.6 ± 2.3

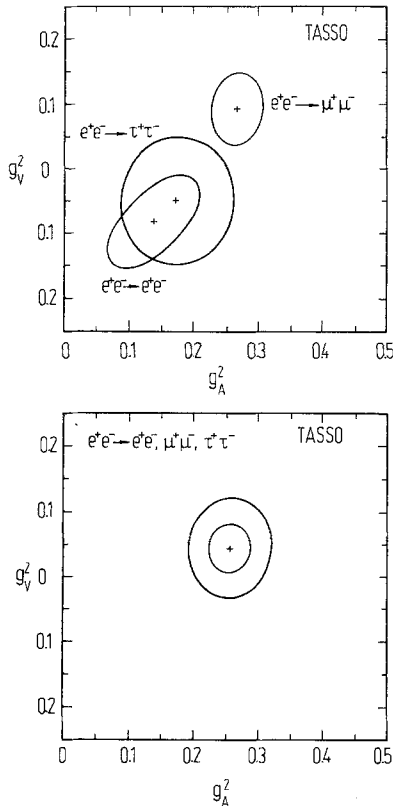


Fig. 3a, b. Results of fits to g_V^2 and g_A^2 . **a** All leptonic reactions separately with 68% confidence level contours, **b** combined analysis for all leptonic reactions with 68% and 90% confidence level contours

likelihood fit to equation 1 the asymmetries extrapolated over the full angular range $-1 \leq \cos \bar{\theta} \leq 1.0$ were derived as given in Table 1. They support the standard model (values denoted by A_{GSW}).

For further analysis we included our previous high energy data at $\sqrt{\langle s \rangle}=34.5$ GeV (note that this analysis contains also 1-1 and 3-3 τ pair topologies). From the asymmetry and total cross section measurements we found for the product of the vector and axial vector couplings

$$g_V^e \cdot g_V^\tau = -0.049 \pm 0.098,$$

$$g_A^e \cdot g_A^\tau = 0.175 \pm 0.088.$$

The results are displayed in the $g_V^2 - g_A^2$ plane of Fig. 3a. Taking $g_A^e = -0.498 \pm 0.027$ from $v-e$ scattering experiments [13] the τ axial vector coupling was determined as $g_A^\tau = 0.351 \pm 0.179$.

Table 3. Lower limits (95% confidence level) on mass scale parameters Λ in contact interactions for left-handed (L), right-handed (R), vector (V), and axial vector (A) couplings from the reaction $e^+e^- \rightarrow \tau^+\tau^-$

Coupling	Λ_+ [TeV]	Λ_- [TeV]
LL	1.1	1.3
RR	1.1	1.3
VV	2.3	1.8
AA	1.5	2.6

The data have also been used to search for phenomena beyond the standard model, e.g. compositeness, substructure or new currents, which manifest themselves as residual contact interactions. A general scheme with helicity conserving currents interfering with the photon and Z^0 fields has been given by [15]. Assuming a coupling strength of $g^2/4\pi=1$ the mass scale Λ is the only free parameter. Restricting to pure left-handed, right-handed, vector and axial vector currents lower limits on Λ_{\pm} were derived for two different metrics as summarized in Table 3. They are typically between 1.1 and 2.6 TeV depending on the assumed chiral structure. The traditional QED form factor is a special case of a vector current with electromagnetic coupling, $A^{\text{QED}} \sim \sqrt{\alpha} \cdot A^{\text{VV}}$. We found lower limits (95% confidence level) of $\Lambda_+^{\text{QED}} > 184$ GeV and $\Lambda_-^{\text{QED}} > 221$ GeV.

8 Combined analysis of electroweak parameters

We now compare the TASSO results from all leptonic reactions $e^+e^- \rightarrow \tau^+\tau^-$, $e^+e^- \rightarrow \mu^+\mu^-$ [7], and $e^+e^- \rightarrow e^+e^-$ [16] and perform a combined analysis of electroweak parameters.

In the context of a general $SU(2)_L \times U(1)$ electroweak theory the vector and axial vector couplings can be treated as free parameters. A χ^2 fit to the differential cross sections was performed taking the overall normalisation of each kind of lepton and each energy set as free parameters and let them vary within their systematic uncertainties. The results are shown in the $g_V^2 - g_A^2$ plane of Fig. 3a. Both couplings are almost independent from each other in τ pair and μ pair production, whereas they show a strong correlation (coefficient ~ 0.5) in Bhabha scattering due to the large t channel contribution. The results from the three reactions are compatible with each other supporting the concept of lepton universality.

For the following analysis we will assume lepton universality, i.e. $g_V = g_V^e = g_V^\mu = g_V^\tau$ and $g_A = g_A^e = g_A^\mu$

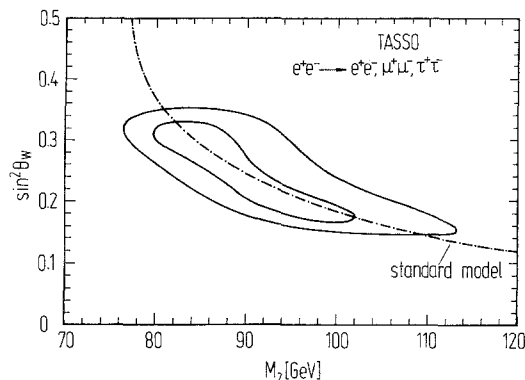


Fig. 4. Regions at 68% and 95% confidence level for $\sin^2 \theta_W$ and M_Z allowed by the combined leptonic data. The dashed line shows the prediction of the standard model

$= g_A^\tau$. A combined fit, shown in Fig. 3b, gave the results

$$g_V^2 = 0.044 \begin{matrix} +0.041 \\ -0.037 \end{matrix},$$

$$g_A^2 = 0.257 \begin{matrix} +0.033 \\ -0.031 \end{matrix},$$

in good agreement with the standard model.

Alternatively, one may keep the standard model weak isospin assignments and treat the coupling strength, $\sin^2 \theta_W$, and the Z^0 mass as free parameters. However, there is a strong correlation of both values, as shown in Fig. 4. Thus e^+e^- data can only be used to check the consistency between $\sin^2 \theta_W$ and M_Z measurements in different experiments. Taking $M_Z = 91.9 \pm 1.8$ GeV from collider experiments [12] we obtain

$$\sin^2 \theta_W = 0.211 \begin{matrix} +0.039 + 0.021 \\ -0.021 - 0.015 \end{matrix},$$

where the second error comes from the Z^0 mass uncertainty. This value is consistent and comparable in precision with those obtained from purely leptonic neutrino electron scattering experiments. Conversely, fixing $\sin^2 \theta_W = 0.226 \pm 0.007$ [13] we get $M_Z = 90.9 \pm_{-3.9}^{+4.6}$ GeV, to be compared with the standard model expectation of $M_Z = 38.69/\sin \theta_W \cdot \cos \theta_W = 92.5 \pm 1.0$ GeV, assuming a top quark mass of 45 GeV [13].

9 Summary

We have measured the cross section and forward backward charge asymmetry for the reaction e^+e^-

$\rightarrow \tau^+ \tau^-$ at $\sqrt{s} = 35.0$ GeV and $\sqrt{\langle s \rangle} = 42.4$ GeV. Our results support the predictions of the standard model and are in good agreement with our previous measurements as well as with other experiments working at these energies [17]. Including our data from μ pair production and Bhabha scattering we derived improved values for leptonic electroweak parameters. New lower limits on mass scale parameters of hypothetical contact interactions have been reported.

Acknowledgements. We gratefully acknowledge the support of the DESY directorate, the PETRA machine group and the DESY computer center. Those of us from outside DESY wish to thank the DESY directorate for the hospitality extended to us.

References

1. TASSO Coll., M. Althoff et al.: Z. Phys. C – Particles and Fields 26 (1985) 521
2. S.L. Glashow: Nucl. Phys. 22 (1961) 579; Rev. Mod. Phys. 52 (1980) 539; A. Salam, Phys. Rev. 127 (1962) 331; Rev. Mod. Phys. 52 (1980) 525; S. Weinberg, Phys. Rev. Lett. 19 (1967) 1264; Rev. Mod. Phys. 52 (1980) 515
3. TASSO Coll., R. Brandelik et al.: Phys. Lett. 110B (1982) 173
4. TASSO Coll., M. Althoff et al.: Z. Phys. C – Particles and Fields 22 (1984) 13
5. P.E.L. Clarke: D. Phil Thesis, Oxford University, RAL T 024 (1985)
6. C. Balkwill: D. Phil Thesis, Oxford University, RAL T 068 (1988)
7. TASSO Coll., W. Braunschweig et al.: Z. Phys. C40 (1988) 163; (Note: In this reference the second column of Table 2, p. 168, giving the differential cross section at 34.5 GeV, should be inverted.)
8. F.A. Berends, R. Kleiss, S. Jadach: Nucl. Phys. B202 (1982) 63
9. M. Böhm, W. Hollik: Phys. Lett. 139B (1984) 213
10. Particle Data Group, Review of Particle Properties: Phys. Lett. 170B (1986) 1
11. A. Böhm: Proc. xiv ème Rencontre de Moriond (1984) Vol 1, p. 191
12. UA2 Coll., R. Ansari et al.: Phys. Lett. 186B (1987) 440; UA1 Coll., G. Arnison et al.: Phys. Lett. 166B (1985) 484
13. U. Amaldi et al.: Phys. Rev. D36 (1987) 1385
14. G.L. Fogli, D. Haidt: Z. Phys. C – Particles and Fields 40 (1988) 379
15. E.J. Eichten, K.D. Lane, M.E. Peskin: Phys. Rev. Lett. 50 (1983) 811
16. TASSO Coll., W. Braunschweig et al.: Z. Phys. C – Particles and Fields 37 (1988) 171
17. CELLO Coll., H.-J. Behrend et al.: Phys. Lett. 114B (1982) 282; JADE Coll., W. Bartel et al.: Z. Phys. C – Particles and Fields 30 (1986) 371; MARK J Coll., B. Adeva et al.: Phys. Lett. 179B (1986) 177; PLUTO Coll., Ch. Berger et al.: Z. Phys. C – Particles and Fields 28 (1985) 1; HRS Coll., K.K. Gan et al.: Phys. Lett. 153B (1985) 116; MAC Coll., E. Fernandez et al.: Phys. Rev. Lett. 54 (1985) 1620; MARK II Coll., M.E. Levi et al.: Phys. Rev. Lett. 51 (1983) 1941; S.L. Olsen (TRISTAN results), Proc. xxiv. Int. Conf. on High Energy Physics, Munich (1988), p. 868